Electronic Supplementary Material (ESI) for Nanoscale.

Supporting Information

Boosting the Sensitivity with Time-Gated Luminescence Thermometry Using a Nanosized Molecular Cluster-Aggregate

Diogo A. Gálico[†], Muralee Murugesu[†]*

†Department of Chemistry and Biomolecular Sciences, University of Ottawa, Ottawa, Ontario K1N 6N5, Canada.

*Corresponding Author: M. Murugesu (E-mail: m.murugesu@uottawa.ca)

Figures and Tables:

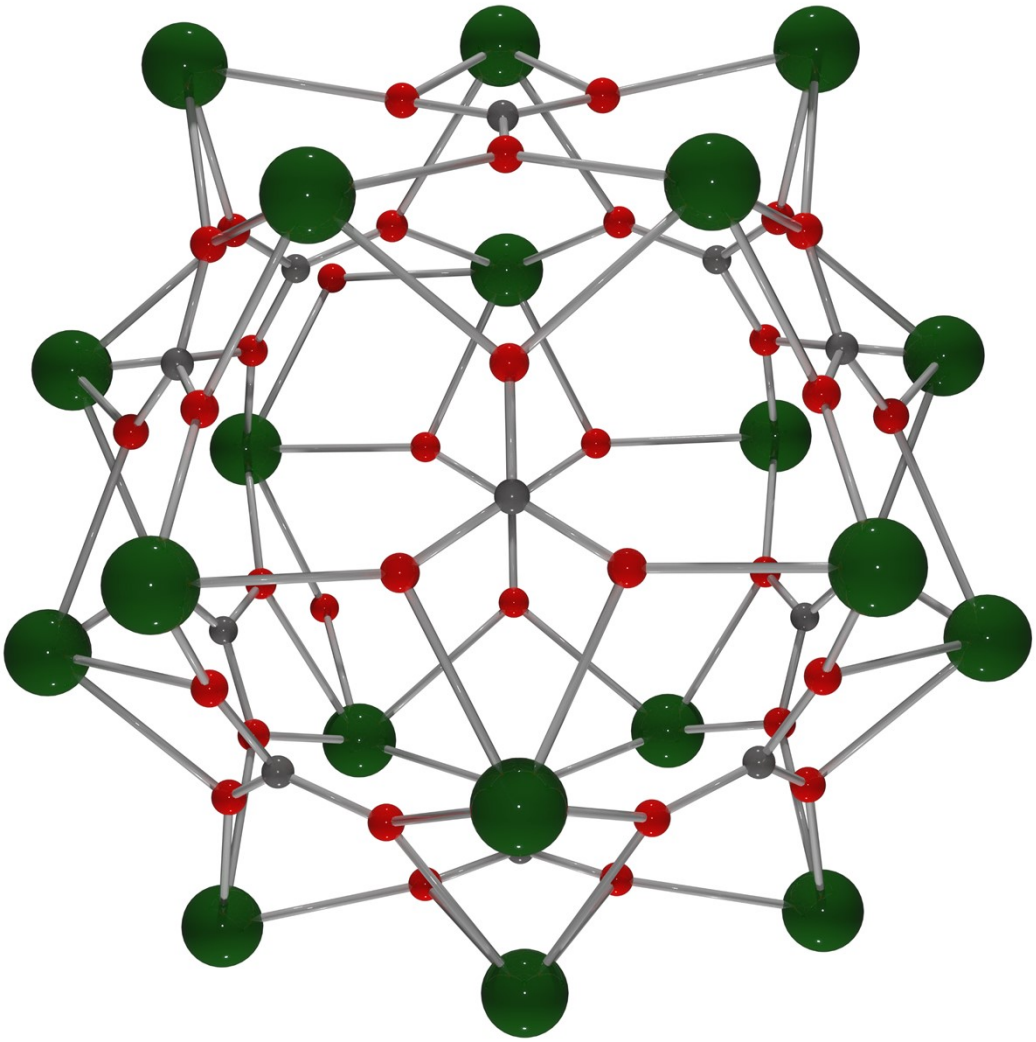

Figure S1. Molecular core structure of the **{Ln_{20}}** MCA viewed along the crystallographic axes *c* (CCDC number: 2023789). Organic ligand, hydrogen and solvent atoms are omitted for clarity. Color code: Green for terbium, gray for carbon, and red for oxygen.

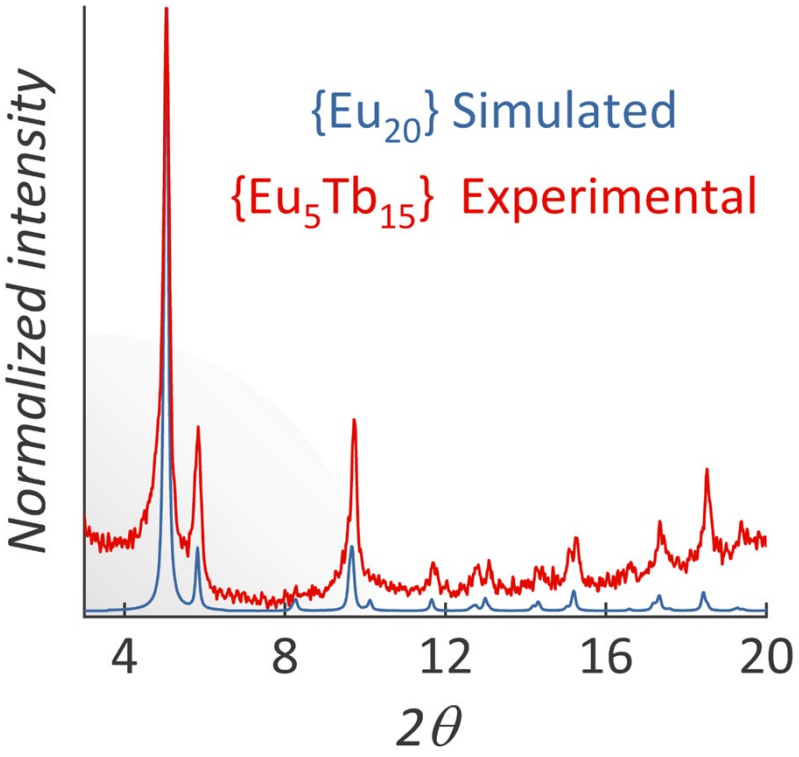

Figure S2. Simulated and experimental PXRD patterns for **{Eu_5Tb_{15}}** MCA. Simulated diffractogram refers to **{Eu_{20}}** MCA (CCDC number: 2023766).

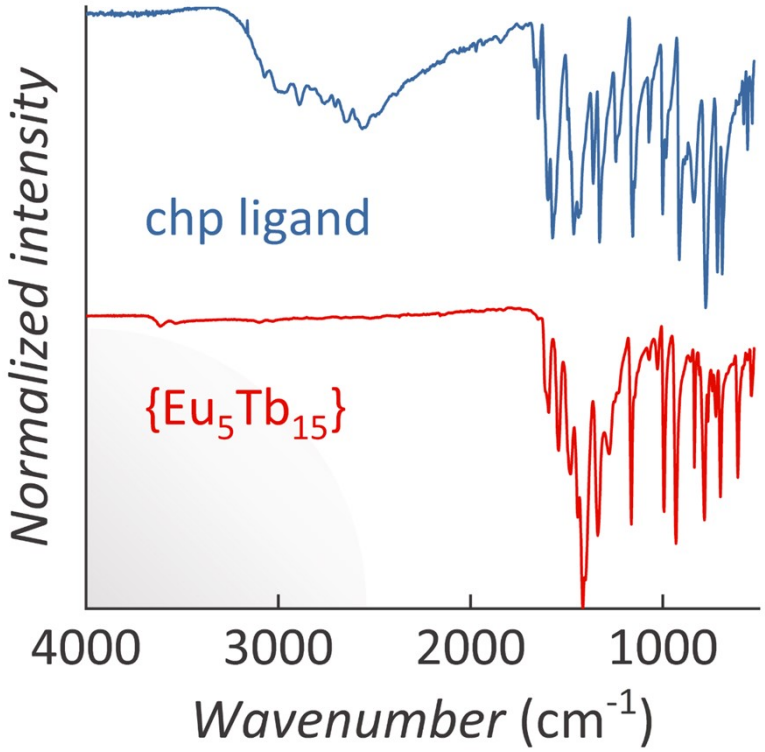

Figure S3. FTIR spectra for chp ligand and **{Eu_5Tb_{15}}** MCA.

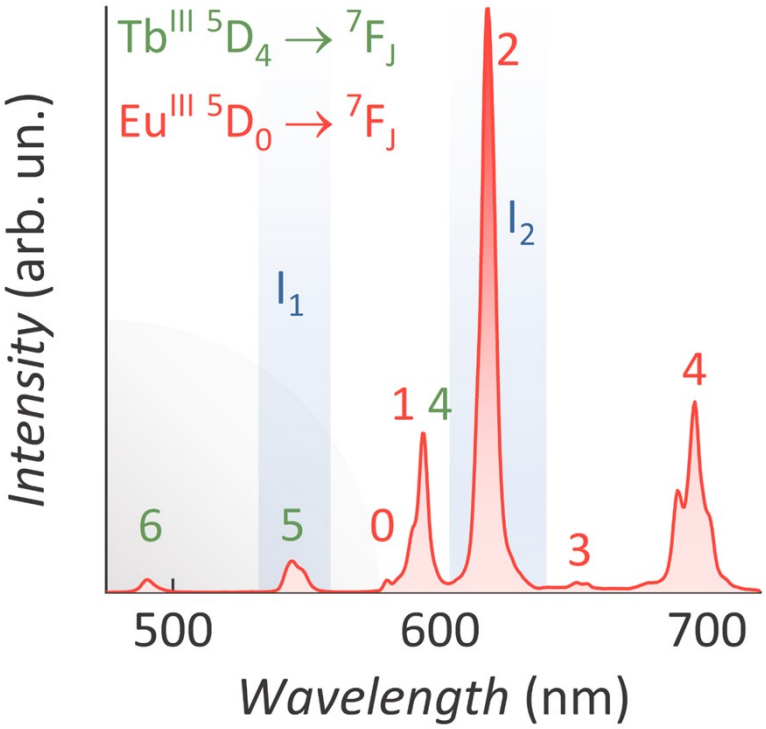

Figure S4. Continuous emission spectrum for a 0.1 g mL^{-1} acetonitrile solution of **{Eu_5Tb_{15}}** MCA obtained at 25 °C. Transitions and integrated areas (I_1 and I_2) for the thermometry studies are labelled.

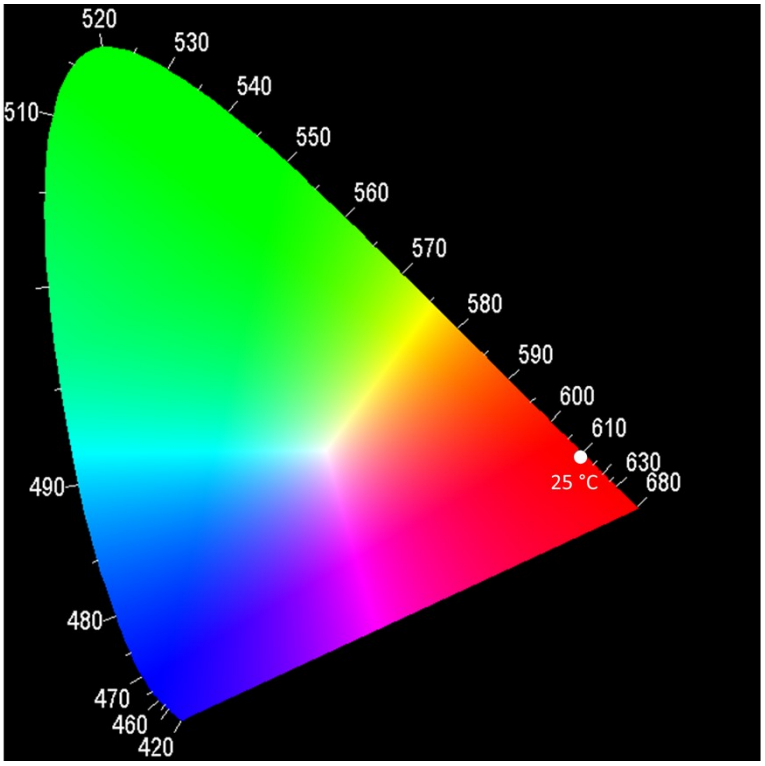

Figure S5. CIE diagram for the continuous emission spectrum showing the predominant red color at 25 °C.

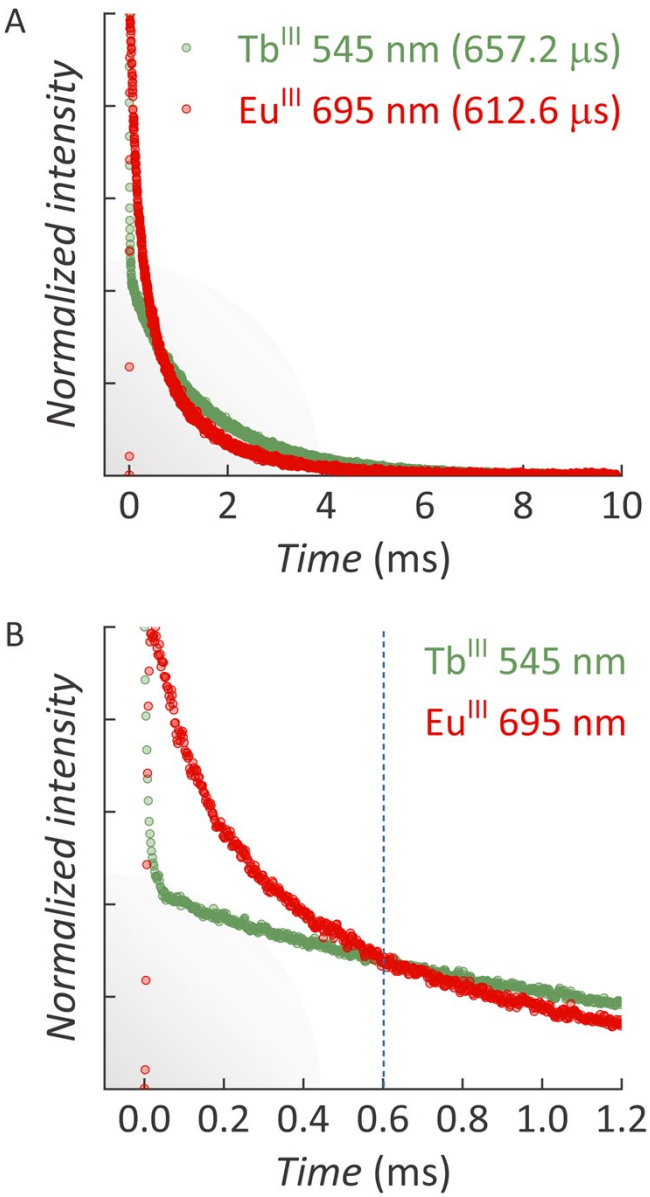

Figure S6. (a) Decay curves displayed in linear scale obtained at 25 °C monitoring Tb^{III} and Eu^{III} components (λ_{ex} = 312 nm). (b) Magnification of the 0 – 1.2 ms range.

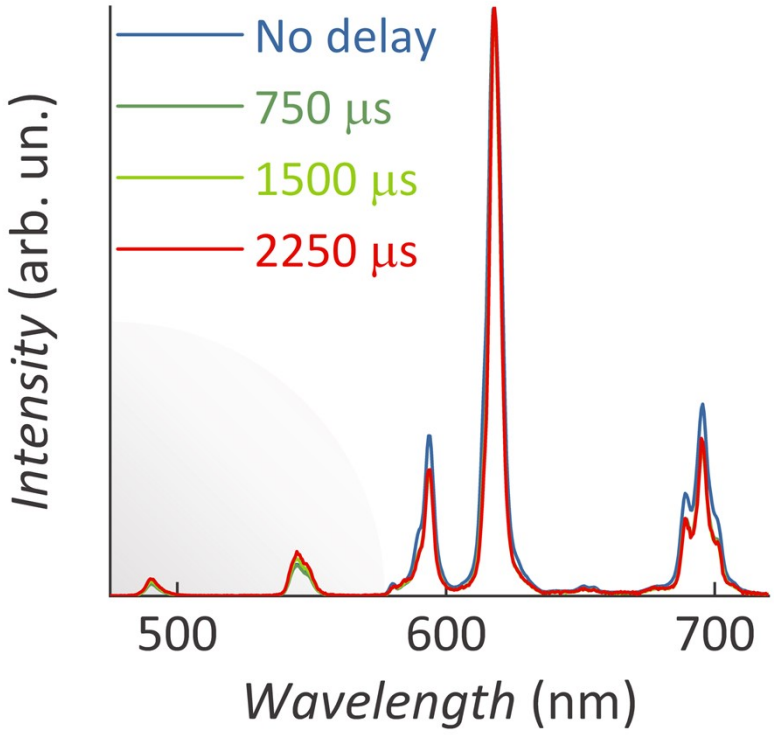

Figure S7. Time-gated emission spectra obtained at 20 °C for **{Eu_5Tb_{15}}**.

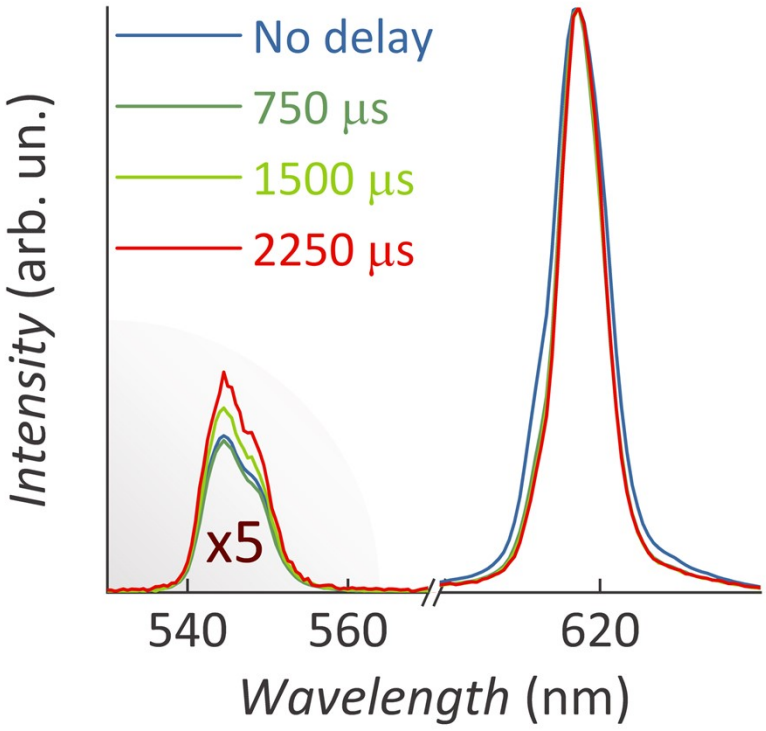

Figure S8. Magnification of the most intense transitions for Tb^{III} and Eu^{III} ions (same data from the figure S6). Tb^{III} components were multiplied to facilitate the visualization.

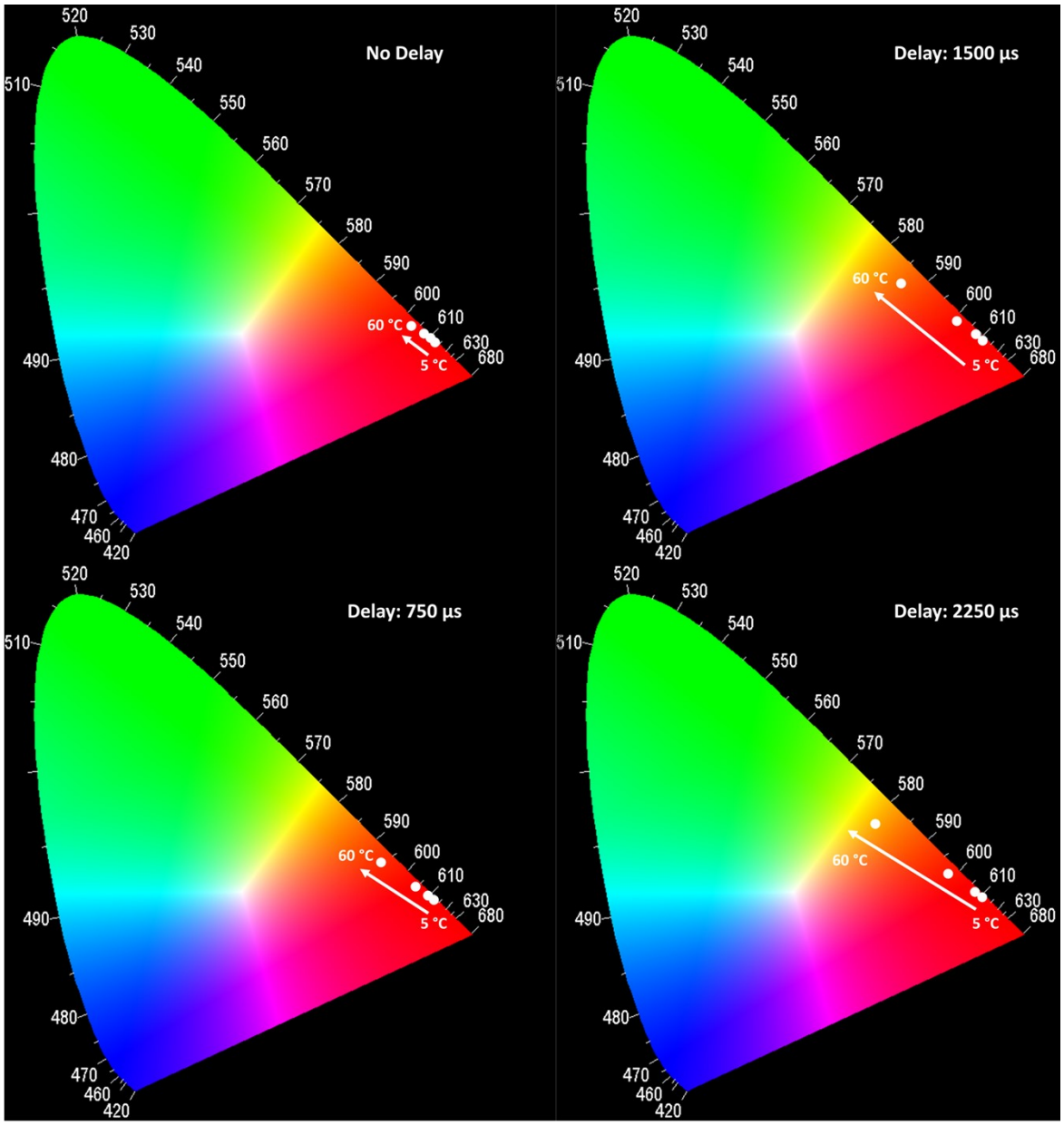

Figure S9. CIE diagram for the time-gated temperature-dependent emission spectra highlighting the coordinates at 5, 20, 40, and 60 °C.

Table S1. Best-fitting parameters for the thermometric parameter (Δ).

Detection delay	A_1	A_2	X_0	r^2
0	46.211	-5.490	-1.093	0.999
750	42.252	-2.158	5.086	0.999
1500	34.561	-1.284	6.931	0.999
2250	30.273	-0.995	7.823	0.999

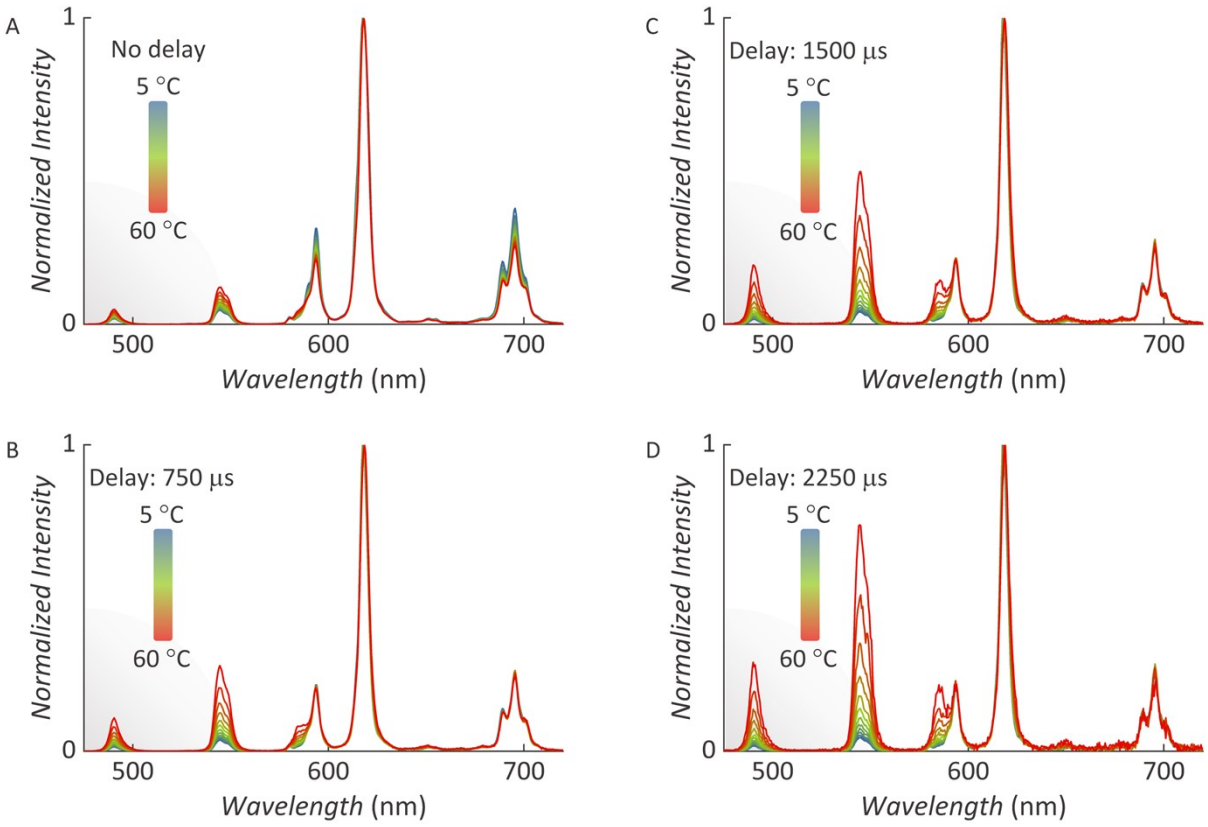

Figure S10. Normalized temperature-dependent time-gated emission spectra for **{Eu_5Tb_{15}}** with λ_{ex} = 312 nm (a) without a detection delay and with detection delays of (b) 750, (c) 1500, and (d) 2250 µs. Temperature step interval: 5 °C. (same data from Figure 2).

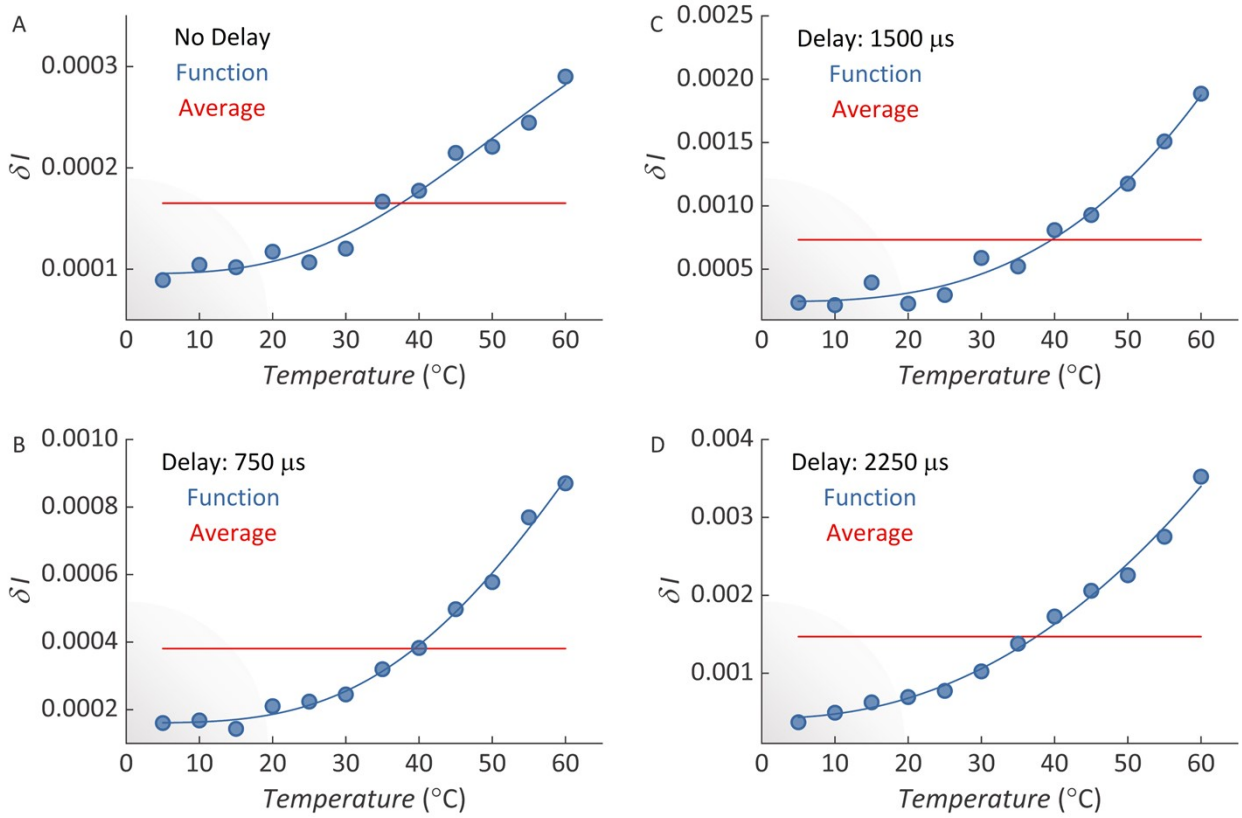

Figure S11. Signal fluctuations obtained *via* a temperature-dependent function (best-fit parameters in Table S2) and *via* the commonly used average method. To model the experimental data, a logistic function as implemented in OriginPro 2021 was used.

Table S2. Best-fitting parameters for the signal fluctuation function (δI).

Detection delay	**A_1**	**A_2**	**X_0**	**p**	**r^2**
0	8.56×10^{-5}	4.94×10^{-4}	62.59	3.04	0.977
750	1.61×10^{-4}	3.17×10^{-3}	85.26	3.29	0.994
1500	2.45×10^{-4}	1.44	618.67	2.91	0.983
2250	4.23×10^{-4}	55.14	4974.39	2.22	0.992